

Chemical Vapor Deposition of Aluminosilicates from Mixtures of SiCl₄, AlCl₃, CO₂, and H₂

Stephanos F. Nitodas^{a,*} and Stratis V. Sotirchos^{a,b,**,z}

^aDepartment of Chemical Engineering, University of Rochester, Rochester, New York 14627, USA

^bInstitute of Chemical Engineering and High Temperature Chemical Processes, 265 00 Patras, Greece

A comprehensive study of the chemical vapor codeposition of silica, alumina, and aluminosilicates from SiCl₄-AlCl₃-H₂-CO₂ mixtures is presented. A hot-wall reactor, coupled to an electronic microbalance, is used to investigate the dependence of the deposition rate on temperature, pressure, composition, and total flow rate over a broad range of operating conditions. The experimental observations are discussed in the context of the results obtained in independent deposition experiments of silica and alumina from mixtures of SiCl₄-H₂-CO₂ and AlCl₃-H₂-CO₂, respectively, in the same apparatus. The results show that the deposition of silica proceeds at very low rates that are by more than an order of magnitude lower than those of alumina deposition at the same temperature, pressure, total flow rate, and carbon dioxide and chloride mole fractions in the feed. When both chlorides (SiCl₄ and AlCl₃) are fed to the reactor, that is, in the codeposition process, the rate of SiO₂ deposition is much higher than that seen in the single species deposition experiments, while the opposite behavior is observed for the rate of deposition of Al₂O₃. The results of deposition experiments conducted on refractory wires, in order to obtain information on the effect of the substrate position in the reactor, show that manipulation of residence time offers a way to control the composition of the codeposited films in alumina and silica. The experimental results are compared with those obtained in a past study using methyltrichlorosilane as silicon source.

© 2000 The Electrochemical Society. S0013-4651(99)02-031-5. All rights reserved.

Manuscript submitted February 5, 1999; revised manuscript received September 9, 1999.

The preparation of films of metal oxides is of interest for a number of applications, such as high-temperature gas separations, protection of metals and other materials from corrosion and oxidation, heterogeneous catalysis, and microelectronics.¹⁻⁴ An important application of inorganic oxides is in the field of structural applications, where they find use as coatings for the protection of metals and other materials from high-temperature corrosion caused by combustion gases and trace contaminants. Because of their high hardness and excellent corrosion resistance, alumina and zirconia are very attractive for use as coatings for wear and corrosion protection.³⁻⁶ Mullite (3Al₂O₃·2SiO₂) also possesses very attractive properties for structural applications.⁷ Its thermal expansion coefficient is lower than those of alumina and zirconia and similar to that of Si-based ceramics (e.g., silicon carbide). As a result, it is suitable for application on SiC components that are subjected to thermal cycling in the course of their usage.

Several methods can be used for the preparation of inorganic oxides, such as thermal oxidation, sol-gel processing, and chemical vapor deposition. Because of their low cost, metal chlorides are the most frequently used metal sources for the chemical vapor deposition of metal oxides. An extensive amount of work has been done on the chemical vapor deposition of Al₂O₃ through the oxidation or hydrolysis of AlCl₃,^{4-6,8-16} but only a few groups have dealt with the deposition of silica,^{17,18} and fewer studies have examined the deposition of mullite.¹⁹⁻²¹ SiCl₄ is typically employed as silicon source in the chemical vapor deposition of silica and mullite.

In a previous study,²² we investigated the chemical vapor codeposition of SiO₂, Al₂O₃, and aluminosilicates from mixtures of CH₃SiCl₃ (methyltrichlorosilane, MTS), AlCl₃, CO₂, and H₂. MTS was used as silicon source because preliminary experiments showed that the rates of deposition of silica and alumina from H₂-CO₂ mixtures containing MTS and AlCl₃, respectively, were of comparable magnitude for similar chloride concentrations, whereas mixtures of SiCl₄, CO₂, and H₂ gave much lower rates of deposition of silica. The experiments revealed that the codeposition process exhibited deposition rates that were not only larger than those of the simple oxides (Al₂O₃ and SiO₂) from MTS and aluminum trichloride, respectively, at the same operating conditions, but also larger than their sum by a factor of two to three. The analysis of the composition of

the deposits showed that the increase in the codeposition rate was accompanied by a dramatic enhancement of the deposition of SiO₂ and a reduction in the rate of Al₂O₃ deposition, the combination of which led to very low Al/Si ratios in the deposits.

In order to obtain higher Al/Si ratios in the codeposited films (corresponding to stoichiometric mullite or alumina-rich mullite), it is necessary to suppress the enhancement of SiO₂ deposition and maintain the rate of Al₂O₃ deposition at least at the levels seen in the absence of silicon precursors from the feed. Since the rate of SiO₂ deposition in the codeposition process is much higher than the rate of silicon deposition in the absence of AlCl₃, it is evident that it is the interaction of aluminum and silicon precursors that is responsible for the enhanced deposition rate of silica and hence, the enhanced codeposition rate. If the silicon surface species involved in the fast deposition steps are the same as those that lead to silicon deposition in the single species deposition process, it is possible to lower the rate of silica deposition in the codeposition process by employing a silicon precursor that exhibits a much lower rate of SiO₂ deposition than MTS, such as SiCl₄.

The preparation of alumina, silica, and aluminosilicate (e.g., mullite) coatings through chemical vapor deposition from mixtures of AlCl₃, SiCl₄, CO₂, and H₂ is the subject of the present study. Deposition experiments are carried out in a gravimetric, hot-wall chemical vapor deposition (CVD) reactor over a wide range of operational conditions in order to determine the dependence of the codeposition and single-species deposition rates on temperature, pressure, flow rate, and feed composition. The effect of the substrate position in the reactor on the deposition rate and deposit composition is also studied by conducting experiments on thin refractory wires placed along the center line of the reactor. The results are compared with those obtained with MTS as silicon source and discussed in the context of past studies on silica, alumina, and aluminosilicate deposition and on the basis of the results of thermodynamic equilibrium computations.

Experimental

CVD experiments were carried out in a vertical hot-wall reactor made of quartz with a 15 mm internal diameter. The reactor is coupled to an electronic microbalance (1 µg sensitivity) for continuous monitoring of the weight of the deposit. Aluminum trichloride is formed *in situ* in a packed-bed reactor (chlorinator) loaded with high-purity aluminum granules and kept at a temperature above 250°C in order to achieve complete conversion of HCl to AlCl₃.⁴ The pressure in the deposition chamber is measured at the inlet of

* Electrochemical Society Student Member.

** Electrochemical Society Active Member.

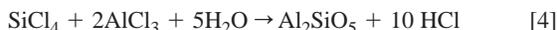
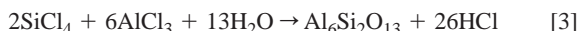
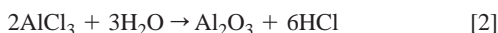
^z E-mail: svs2@che.rochester.edu

the reactor using a capacitance manometer, and it is regulated by a throttling valve controlled by a pressure controller. Subambient pressures are generated using a mechanical vacuum pump. The pump and the control valve are protected by using a liquid nitrogen trap, a soda-lime trap, and a particulate filter. The reactor tube and the substrate are heated with a high-temperature single-zone resistance furnace, which provides about 25 cm (10 in.) of heating zone. Temperature measurements in the reactor showed that the part of the reactor tube that lies in the heating zone is almost isothermal,²³ with the temperature being within $\pm 5^\circ\text{C}$ of the set-point value.

Local deposition rates were measured using small silicon substrates (typically, 1.35 cm length, 0.75 cm width, and 0.20 mm thickness) obtained by depositing silicon from mixtures of silicon tetrachloride and hydrogen on substrates made of high-density graphite blocks. The substrates were hung from the sample arm of the microbalance and placed within the heating zone, with the deposition surface parallel to the flow of the reactive mixture, which enters the chemical reactor from the top. Experiments were also carried out on thin molybdenum wires placed along the center line of the tubular reactor in order to obtain information on the profiles of deposition rate and deposit composition along the reactor. At each set of experimental conditions, the deposition process was allowed to occur for a period of time that was sufficient to extract a reliable deposition rate from the slope of the weight vs. time curve.

Results and Discussion

The overall reactions that describe the deposition of silica, alumina, and aluminosilicates (*e.g.*, $\text{Al}_6\text{Si}_2\text{O}_{13}$ and Al_2SiO_5) are



The overall reaction for the formation of water vapor is the water gas-shift reaction



These reactions do not represent what actually occurs in the CVD reactor. The deposition process involves many homogeneous and heterogeneous reactions in which many gas-phase species and species adsorbed on the deposition surface participate. The deposition rate at a certain location in the chemical reactor is determined by the concentrations of the various species that take part in the heterogeneous reactions that lead to solid deposition. These concentrations are in turn determined not only by the composition of the feed but also by the flow field in the chemical reactor and the rates of the other chemical reactions that take place in the reactor. The chemical reactor we use in this study has length much larger than its diameter, and thus, it is characterized by a simple flow field, which permits its operation to be described by a simple plug flow model. However, the interpretation of the various effects that are revealed by the experimental data still requires consideration of what the reactive mixture experiences before it reaches the deposition surface.

Most of the results that we present in this study were obtained using mixtures of AlCl_3 and (or) SiCl_4 in H_2 , and CO_2 with $300\text{ cm}^3/\text{min}$ total flow rate at 100 Torr total pressure. The substrates were placed with their midpoint at a distance of 4 cm from the top of the heating zone of the reactor (0 cm position). The top of the heating zone almost coincided with the beginning of the isothermal zone of the chemical reactor. The values of the operating parameters are reported in the figures for each curve of experimental results shown there.

Temperature effects.—Figure 1 presents typical results on the variation of the deposition rate of the single oxides and of the codeposition rate with the temperature in Arrhenius coordinates, that is, as $\ln R_d$ vs. $1/T$, with R_d being the deposition rate and T the absolute temperature in the reactor. To obtain these results, the temperature

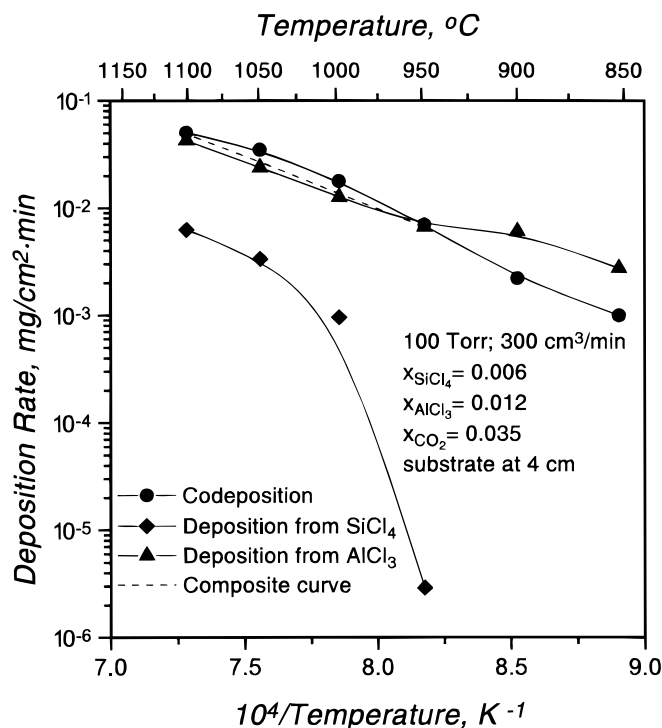


Figure 1. Temperature dependence of deposition and codeposition rates at 100 Torr.

was varied between 850 and 1100°C at 50°C increments. The mole fractions of the source gases were 0.006 SiCl_4 (x_{SiCl_4}), 0.012 AlCl_3 (x_{AlCl_3}), and 0.035 CO_2 (x_{CO_2}). It is seen that the temperature has a positive effect on the deposition rates of all three processes. This effect is stronger in the case of SiO_2 deposition, where the rate varies by more than three orders of magnitude between the lower and the upper temperature limit. When the CVD system operates at 1000°C or above, the deposition of silica proceeds at significant rates. The decrease of the temperature from 1000 to 950°C is followed by a dramatic reduction in the deposition rate. The resulting low values, of the order of $10^{-6}\text{ mg/cm}^2\text{ min}$, lie within the limitations of our microbalance for small-surface-area (nonporous) substrates.

The apparent activation energy (E_{app}), the slope of the $\ln R_d$ vs. $1/T$ curve, decreases with increasing temperature for the case of silica deposition. Linear regression over the entire temperature range in which data are shown in Fig. 1 gives an activation energy value of 71.5 kcal/mol, while a much lower value of 28.5 kcal/mol is obtained when the data at low temperatures ($<1000^\circ\text{C}$) are not included in the calculations. The Arrhenius plot of the alumina deposition process gives an apparent activation energy of 14 kcal/mol. This value is lower than the value (19.6 kcal/mol) that was determined in a past study²² in the same experimental arrangement using different concentrations of aluminum trichloride in the feed ($x_{\text{AlCl}_3} = 0.009$).

The overall deposition rate in the codeposition process changes with the temperature in a similar way as the rate of Al_2O_3 deposition. The Arrhenius plot of the codeposition process (Fig. 1) yields an activation energy of 22.1 kcal/mol. This value is by a factor of three larger than the activation energy reported in Ref. 19 (7.4 kcal/mol), where the chemical vapor deposition of mullite from mixtures of SiCl_4 , AlCl_3 , CO_2 , and H_2 was investigated. The deposition rates that are reported in that study are of the same order of magnitude as those found here. The difference in the apparent activation energies is most probably a reflection of the different reactor configurations and the different operating conditions.

The codeposition rate and the deposition rate of alumina have, in general, comparable values. At temperatures greater than 950°C, the codeposition rate is higher than the deposition rate of alumina, and since the latter is much larger than the deposition rate of silica, high-

er than the sum of the deposition rates that are measured when only one of the two chlorides (AlCl_3 or SiCl_4) is contained in the feed at the same concentration as in the mixture (composite curve in Fig. 1). This is an indication that in the codeposition process aluminum-containing species and silicon-containing species participate in surface reaction steps that lead to solid product deposition at rates that are greater than those of the steps that lead to the deposition of SiO_2 and Al_2O_3 in the independent deposition experiments.

Pressure effects.—The effect of pressure on the reaction rate of the three deposition processes is shown in Fig. 2 at 1000°C and a $\text{CO}_2/(\text{SiCl}_4 + \text{AlCl}_3)$ feed ratio of 2. An increase of the total system pressure is accompanied by an increase in the rate of SiO_2 deposition, with the deposition rate changing by a factor of three between the two limits of the pressure range. The deposition rate of alumina also increases with increasing pressure over the entire pressure range covered in Fig. 2. In contrast to the deposition rates in the single-oxide deposition systems, the deposition rate of the codeposition process displays a complex dependence on pressure. The codeposition rate increases as the pressure moves from 75 to 150 Torr, but then it starts to decrease, reaching a minimum value at 250 Torr. Subsequently, it starts to increase again with the rate at 300 Torr being higher by more than a factor of two than the local minimum rate at 250 Torr.

The negative effect of pressure on the codeposition rate at the range 150-250 Torr is not surprising considering that a rise in the pressure of operation affects various factors which may have qualitatively different effects on the deposition rate. With the feed composition and the temperature kept constant, an increase in the operating pressure increases both the concentrations of the reactants and the residence time in the reactor. Larger concentrations tend to lead, in general, to higher deposition rates, but this effect may be offset by the greater consumption of reactive species and the greater production of product species upstream of the deposition site, because of the increased residence time.

It must be noted that the deposition rate may be negatively influenced by the formation of powder in the reactor, since when this happens, the consumption rates of the gaseous reactants are increased. Insignificant powder formation was observed in our experiments, even at 300 Torr. This observation is consistent with the results of Fig. 2 which show increasing deposition rate with increasing pressure in the upper part of the pressure range where powder formation, if it

occurred, should proceed with higher rate. A reduction in the rate of mullite deposition at pressures higher than 150 Torr was observed in Ref. 19, and was attributed to powder production. Positive influence of pressure on Al_2O_3 deposition was reported by Colmet and Naslain,⁶ who conducted experiments at low aluminum trichloride concentrations ($x_{\text{AlCl}_3} = 0.008$) without detecting occurrence of powder formation even at ambient pressures. Funk *et al.*⁵ noticed a dramatic drop in the deposition rate of Al_2O_3 at pressures above 200 Torr. They attributed it to powder formation even though they used mixtures with low AlCl_3 content ($x_{\text{AlCl}_3} = 0.004$).

Feed composition effects.—Results on the influence of the feed composition on the deposition rate are shown in Fig. 3-6, which present deposition rate vs. reactant mole fraction data for various temperatures. The results of Fig. 3 refer to the effects of SiCl_4 on the deposition rate of silica. It is seen that the operating temperature may affect the dependence of the deposition rate of silica on the mole fraction of SiCl_4 both qualitatively and quantitatively. The effect of the mole fraction of SiCl_4 on the deposition rate of silica changes from negative at 1000°C to positive at 1050°C . At 1100°C , the deposition rate depends weakly on x_{SiCl_4} , presenting a shallow minimum in the lower part of the 0.005-0.04 mole fraction range that is covered in the figure. As in the case of the data reported in Fig. 2, very small amounts of powder were observed at the exit of the reactor. It should be noted that powder formation cannot be the cause of the negative dependence of the deposition rate on the SiCl_4 mole fraction at 1000°C , because this phenomenon, whenever it occurs, tends to intensify with increasing temperature. The complex dependence of the deposition rate of silica on the mole fraction of SiCl_4 most probably reflects the effects of the reaction by-products and, in particular, of HCl. An increase in the SiCl_4 mole fraction in the feed leads not only to higher concentrations of SiCl_4 in the reactor but also to higher concentrations of HCl and of the other by-products of the gas-phase decomposition reactions.

Figure 4 presents results on the dependence of the codeposition rate and the deposition rate of Al_2O_3 in single-oxide deposition experiments on the AlCl_3 mole fraction in the feed at three temperatures (1000, 1050, and 1100°C). The mole fractions of SiCl_4 and CO_2 are 0.006 and 0.035, respectively, but similar results were obtained for other values of these two operating parameters. It is seen that the introduction of small quantities of AlCl_3 in the SiCl_4 - CO_2 - H_2 mixture leads to a steep rise of the deposition rate. A simi-

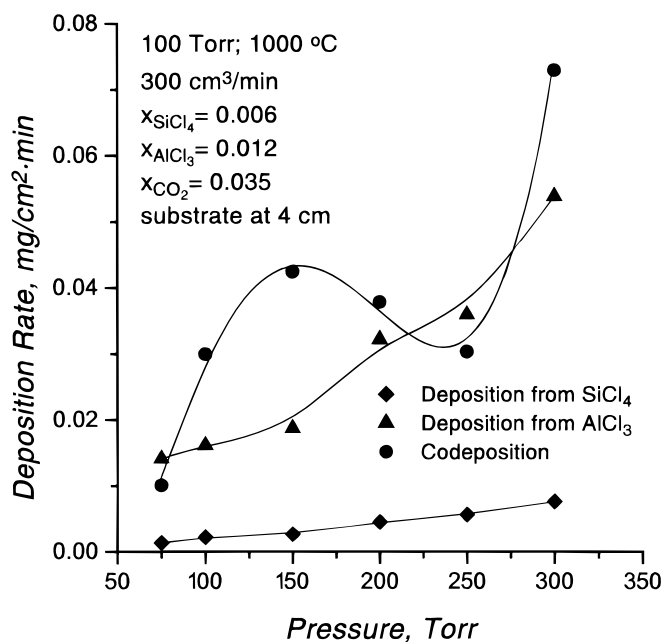


Figure 2. Pressure dependence of deposition and codeposition rates at 1000°C .

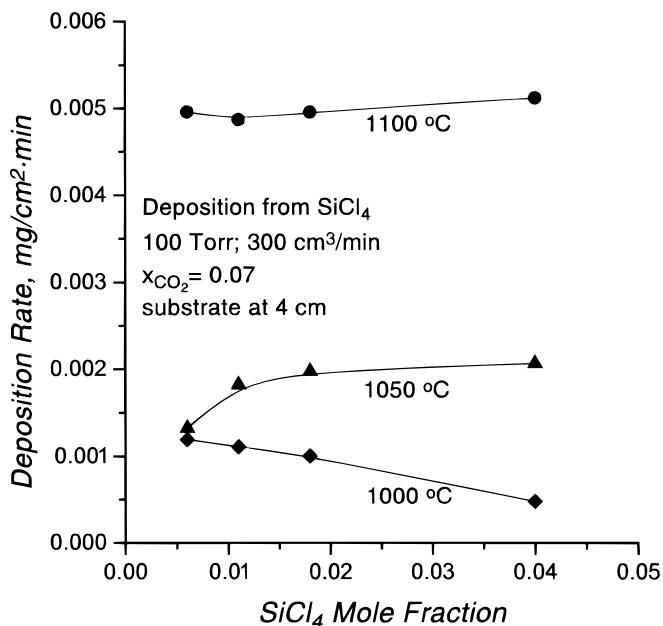


Figure 3. Effects of the SiCl_4 mole fraction on the rate of SiO_2 deposition at 100 Torr and various temperatures.

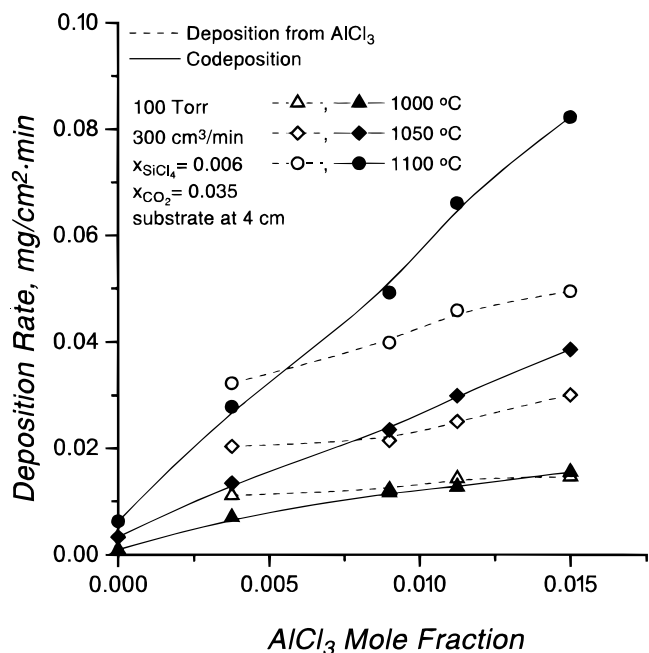


Figure 4. Effects of the AlCl_3 mole fraction on the deposition rate in the presence or absence of SiCl_4 at 100 Torr and various temperatures.

lar observation was made by Auger and Sarin,²⁰ but Mulpuri¹⁹ noticed a precipitous drop in the deposition rate as the Al/Si feed ratio changed from zero to 0.5. As the AlCl_3 feed mole fraction in the feed is increased, both the codeposition rate and the deposition rate of Al_2O_3 from $\text{AlCl}_3\text{-H}_2\text{-CO}_2$ mixtures increase. Enhancement of the codeposition rate with further increase of the Al/Si feed ratio was observed in Ref. 19 after the initial drop, but the opposite behavior was reported in Ref. 20 for experiments conducted in a similar chemical vapor deposition apparatus.

In the lower part of the AlCl_3 mole fraction range covered in Fig. 4, the codeposition process proceeds with lower rate than the deposition of alumina. The AlCl_3 mole fraction value at which the codeposition rate becomes larger than the rate of deposition of alumina decreases with increasing reaction temperature. Experiments at other conditions showed that this value also depends on the feed mole fractions of SiCl_4 and CO_2 . Using the results of Fig. 1 for the deposition rate of silica, one finds that in the upper part of the AlCl_3 mole fraction range of Fig. 4, the codeposition rate is much higher than the sum of the deposition rates of Al_2O_3 and SiO_2 in independent deposition experiments. This was also observed to be the case in Fig. 1 at high temperatures. These results reinforce the conclusion that the surface chemistry of the codeposition process must involve reaction steps that include both silicon species and aluminum species.

Data on the effect of the feed mole fraction of carbon dioxide on the deposition rate of the single oxides and on the codeposition rate are presented in Fig. 5 and 6 at 1000°C for several combinations of mole fractions of chlorides. For the codeposition process, data are also given at 1050°C for 0.6% SiCl_4 and 1.2% AlCl_3 in the feed (Fig. 6). The results show that the feed mole fraction of CO_2 influences the deposition rates of the three processes in a complex way. Depending on the values of the other operating parameters, an increase in the CO_2 mole fraction may increase, decrease, or have no effect on the deposition rate. For the codeposition rate and the deposition rate of alumina, the most common behavior pattern is an initial increase as the CO_2 mole fraction is raised from the lowest value used in experiments (*i.e.*, 0.035) followed by a region on small change or a maximum. For deposition of silica with 0.6% SiCl_4 in the feed, the deposition rate undergoes a small drop as the CO_2 in the feed is changed from 3.5 to 7% and shows little change after that. On the other hand, for 0.011 SiCl_4 mole fraction, it increases continuously, but slowly, as the CO_2 mole fraction is increased.

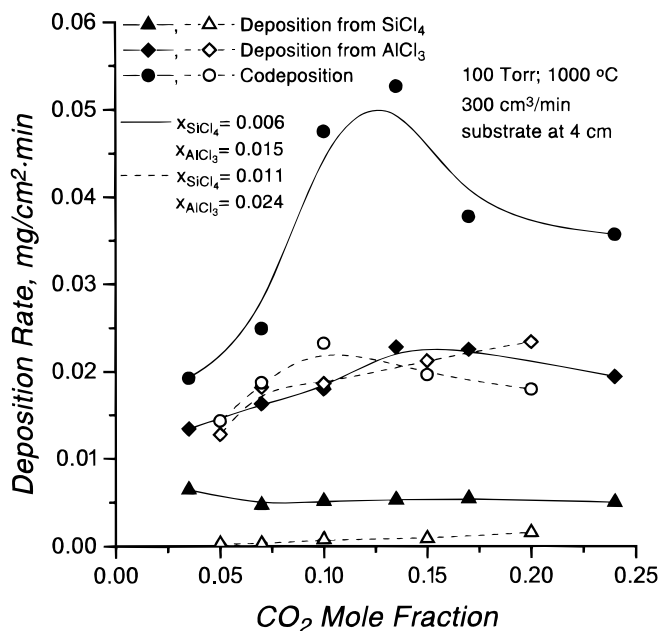


Figure 5. Effects of the CO_2 mole fraction on the deposition and codeposition rates at 100 Torr and 1000°C for two sets of chloride mole fractions.

All codeposition rates vs. CO_2 mole fraction curves in Fig. 5 and 6 present a maximum, which is more pronounced for reaction conditions that give high rates of deposition. The CO_2 mole fraction value at which the maximum occurs lies in the 0.07-0.13 range, and it tends to move toward lower values as the temperature is reduced or as the mole fraction of SiCl_4 is increased. Since these changes lead to lower deposition rates, this behavior suggests that the location of maximum is moved to larger CO_2 mole fractions as the codeposition rate is increased. The appearance of a maximum in the variation of the deposition rate with the CO_2 mole fraction has been observed in many experimental studies on the chemical vapor deposition of alumina from mixtures of AlCl_3 , CO_2 , and H_2 .^{13,16,24}

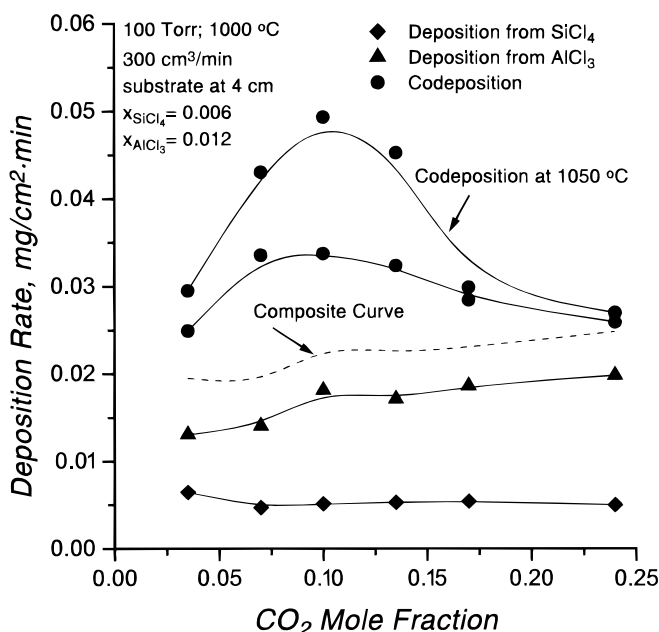


Figure 6. Effects of the CO_2 mole fraction on the deposition and codeposition rates at 100 Torr and 1000°C. Codeposition results are also shown at 1050°C.

The increase in the deposition rate with an increase in the CO_2 mole fraction is most probably caused by the increase in the concentration of H_2O or of other oxygen-donor species with high surface reactivity, such as OH. The appearance of a maximum suggests that the formation of oxygen-donor species ceases to be the rate-limiting step of the overall process above some value of CO_2 concentration. As the mole fraction of CO_2 in the feed is increased, the concentrations of species that contain metal (Si or Al) and oxygen should also increase at the expense of silicon or aluminum species that contain chlorine or hydrogen. For deposition of silicon from SiCl_4 , past studies^{25,26} have shown that SiCl_x are the species that are mainly responsible for Si incorporation in the deposit. If an analogous situation exists in the case of metal incorporation in the deposit during deposition of oxides, that is, SiCl_x and AlCl_x are the main surface reactive species, the reduction in the concentration of metal-chlorine with the increase of the concentration of CO_2 should eventually offset the positive effect of the increase in the concentrations of the oxygen-donor species on the reaction rate. CO_2 appears to affect differently the deposition rate of silica from the deposition rate of alumina and the codeposition rate because the former is considerably lower at similar reaction conditions; therefore, the formation of water and of other oxygen-donor species stops being the controlling step of the deposition process at much lower values of CO_2 concentration.

The results of Fig. 3 showed that the increase of the SiCl_4 mole fraction in the feed has a negative effect on the silica deposition rate at 1000°C . Figure 5 shows that this is also the case for the codeposition rate at this temperature. The aluminum chloride mole fraction is larger in the case with the higher value of SiCl_4 mole fraction, but this parameter does not affect significantly the deposition rate of alumina and the codeposition rate at 1000°C when its value is above 0.01 (see Fig. 4). Because of the decrease that the codeposition rate undergoes as the SiCl_4 mole fraction is changed from 0.006 to 0.011, the codeposition rate and the deposition rate of alumina have comparable values for 1.1% SiCl_4 in the feed, whereas they differ by almost a factor of two at the lower value. It was argued in the presentation of the results of Fig. 3 that the negative effect of the increase of the concentration of SiCl_4 on the deposition rate of silica is most probably a consequence of the increase in the concentration of gas-phase reaction products (such as HCl), which have an inhibitory effect on the solid formation reactions. The results of Fig. 5 suggest that this must also be the case in the codeposition process.

Effects of residence time.—The total flow rate and position in the reactor are the two variables that have the most influence on the residence time of the reactant molecules in the hot zone of the reactor upstream of the substrate. The effect of the total flow rate on the codeposition and the single-species deposition rates is shown in Fig. 7 for two temperatures (1000 and 1050°C), 100 Torr total pressure, and an Al/Si feed ratio of two. As the flow rate changes from 200 to $500\text{ cm}^3/\text{min}$, a dramatic reduction in the rate of silica deposition takes place. Above $500\text{ cm}^3/\text{min}$, the rate decreases only slightly with an increase in the flow rate. Since the mass-transport coefficient increases with increasing velocity of flow of the gaseous mixture over the deposition surface, the negative effect of flow rate on the deposition rate indicates that there are insignificant mass-transport limitations from the bulk of the gas phase to the deposition surface. The increase in the total flow-rate also has a negative effect on the codeposition rate. However, there are regions of flow rate values where the deposition rate tends to increase with increasing flow rate, and this leads to appearance of local maxima in the deposition rate vs. flow rate curve. The negative effect of the flow rate on the codeposition rate becomes stronger as the temperature decreases. A maximum also appears in the variation of the alumina deposition rate with the total flow rate.

Decrease in the deposition rate with increasing total flow rate was observed in a study of SiO_2 particle generation from oxidation of SiCl_4 .²⁷ A similar observation was also made by Klaus *et al.*²⁸ and Wise *et al.*,²⁹ who reported that the growth rate of SiO_2 films formed on silicon surfaces through atomic layer control from SiCl_4

and H_2O using binary reaction sequence chemistry increased significantly with increasing exposure time. For alumina deposition, the decrease of the deposition rate at flow rates higher than $400\text{--}500\text{ cm}^3/\text{min}$ in Fig. 7 is at variance with the behavior seen in Ref. 30, where a square root dependence on the total flow rate was observed. This was construed as an indication of the existence of mass-transport limitations on the deposition process. Park *et al.*¹¹ reported linear decrease of deposition rate of Al_2O_3 with decreasing flow rate from 800 to $300\text{ cm}^3/\text{min}$ at 1050°C . The presence of mass-transport limitations was proposed as an explanation for this behavior. Other observations made in Ref. 11 were insignificant change of the deposition rate for flow rates greater than $800\text{ cm}^3/\text{min}$ and no deposition below $300\text{ cm}^3/\text{min}$. These results are in disagreement with the behavior seen in Fig. 7. The differences are most probably due to the use of a different reactor arrangement from that used in the present study, namely, a vertical cold-wall reactor.

To obtain results on the effects of the position of the substrate on the deposition rate from a single experiment, experiments were carried out on thin molybdenum wires placed along the center line of the reactor. Results on the variation of the codeposition rate with the distance from the entrance of the reactor at 1000°C are given in Fig. 8. Kinetic data are shown in the figure for positions lying within the isothermal zone of the reactor, that is $0\text{--}23\text{ cm}$, and therefore, the changes in the deposition rate reflect changes in the composition of the gaseous mixture and not in the temperature of the reaction. The variation of the codeposition rate with the distance in the reactor presents a maximum at about the middle of the isothermal zone of the reactor. This behavior is in agreement with that seen in Fig. 7 for the effects of flow rate. [It must be noted that deposition rate measurements conducted at the same distance from the entrance of the reactor on different substrates (walls of the reactor, plates, and wires) showed small differences among the various substrates. This is a further indication of the absence of significant mass-transport limitations at the conditions of our experiments.] The appearance of the maximum in the variation of the deposition rate of alumina and in the codeposition rate with the residence time is most probably the result of the interaction of the formation of surface reactive species, the depletion of the species in the deposition reactions, and the formation of reaction by-products that have inhibitory effects on solid formation reactions (*e.g.*, HCl). This interaction must also be taking place in the

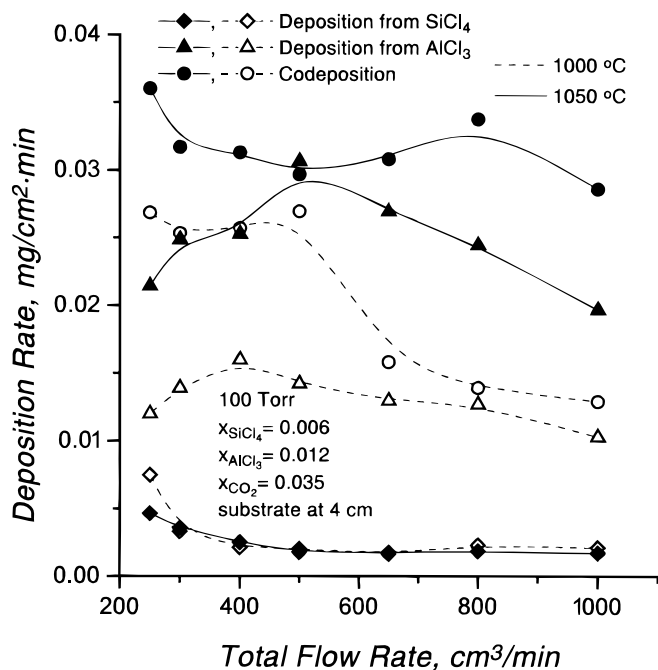


Figure 7. Deposition rate vs. total flow rate for the deposition and codeposition processes at 100 Torr and 1000 and 1050°C .

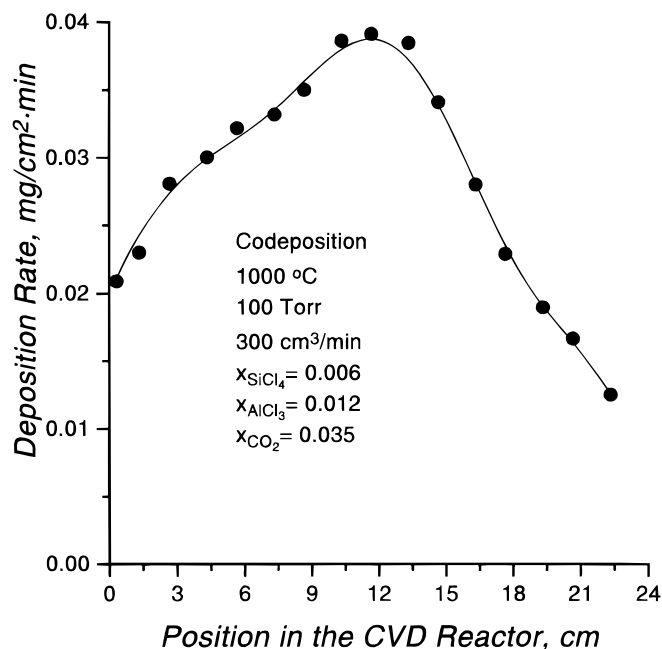


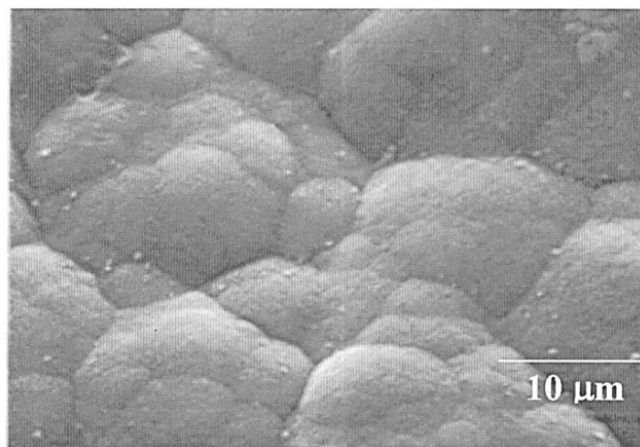
Figure 8. Deposition rate vs. position in the CVD reactor for the codeposition process at 100 Torr and 1000°C.

case of silica deposition, but because of the much lower values of deposition rate, the maximum deposition rate probably occurs at flow rates below the lower limit of the range covered in Fig. 7.

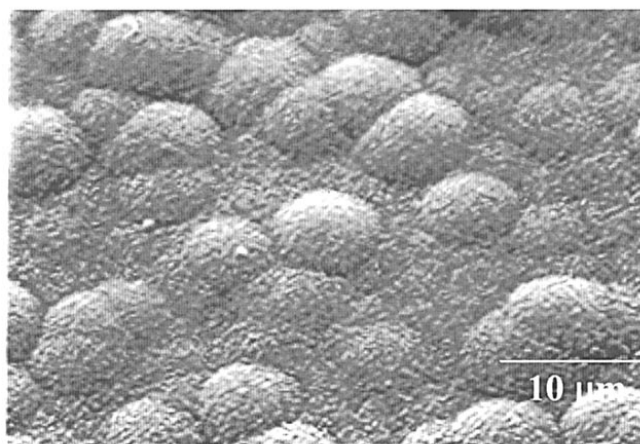
Deposit composition and morphology.—The composition and morphology of the deposits were examined employing energy dispersive X-ray analysis (EDXA) and scanning electron microscopy (SEM), respectively. X-ray diffraction (XRD) analysis revealed that the films of pure alumina consisted of polycrystalline κ - and θ - Al_2O_3 ,²² whereas the silica films were amorphous. Films deposited from SiCl_4 - AlCl_3 - CO_2 - H_2 mixtures were dense and uniform in thickness. Several codeposited films were analyzed with XRD, and for deposition temperatures above 1000°C, they were found to be a mixture of an amorphous component and κ - and θ - Al_2O_3 . The alumina peaks in the codeposits were rather weak in comparison to the peaks seen in pure alumina deposits, suggesting that the amounts of crystalline Al_2O_3 were small and that significant amounts of Al_2O_3 were incorporated into amorphous aluminosilicates. No crystalline phase was detected in deposits obtained at temperatures lower than 1000°C.

Figure 9 shows SEM micrographs of codeposited films formed at 4 cm location, 100 Torr, 300 cm^3/min total flow rate, 0.006 SiCl_4 mole fraction, 0.012 AlCl_3 mole fraction, 0.035 CO_2 mole fraction, and two deposition temperatures (1000 and 1100°C). It is seen that the macroscopic morphology of the surface of the deposits is of nodular structure. The average nodule size decreased slightly as the temperature was changed from 1000 to 1100°C (compare Fig. 9a and b), and the surface of the deposit became rougher and similar to that of pure alumina deposits. The analysis of the composition of the deposits (see below) revealed that this change was accompanied by an increase in the aluminum content of the deposit.

The composition of the deposits was analyzed by EDXA. Since the deposition of alumina proceeds at much higher rates than the deposition of silica (Fig. 1), one would expect that if the two oxides (SiO_2 and Al_2O_3) were deposited in the codeposition process at rates proportional to those seen in the independent deposition experiments at the same operating conditions, Al_2O_3 would be the main component of the codeposited films, especially at low temperatures (<1000°C) where the codeposition rate is comparable to that of alumina. However, the results showed that SiO_2 was the main constituent of the deposit in the entire temperature range, suggesting that the incorporation of silica in the codeposit is more favored than



(a)



(b)

Figure 9. SEM micrographs of CVD films at 100 Torr, $x_{\text{SiCl}_4} = 0.006$, $x_{\text{AlCl}_3} = 0.012$, substrate at 4 cm, and 300 cm^3/min total flow rate. Deposition temperature: (a) 1000 and (b) 1100°C.

that of alumina. From the values of the codeposition rate and the film composition in SiO_2 and Al_2O_3 , the rates of incorporation of the oxides in the codeposited films were computed as functions of temperature, and the results are shown in Fig. 10. The comparison of the alumina and silica deposition rates in the codeposition process and in the single-oxide deposition experiments shows that the codeposition process is followed by a dramatic enhancement of the deposition of silica and an equally dramatic reduction of alumina deposition. As a result, the Al/Si ratio in the deposit is by a few orders of magnitude lower than the ratio expected on the basis of the deposition rates of silica and alumina in single-oxide experiments at the same conditions (compare dashed and solid curves in Fig. 10).

An increase in the reaction temperature has a positive effect on the content of the codeposited films in Al in Fig. 10, but the opposite effect is observed for the Al/Si ratio that is predicted on the basis of the single-oxide deposition experiments. Increasing Al/Si ratio of the deposit with increasing temperature was also reported in Ref. 19, where it was also observed that the deposition rate and the aluminum content of the deposit increased with increasing deposition time. Insignificant variation of the composition of the deposit and of the deposition rate with time was observed in the present study, and a similar observation was made in our past study of aluminosilicate deposition using MTS as silicon source.²²

Figure 11 presents the variation of the Al/Si ratio along the length of the reactor for the film formed on a refractory wire at the condi-

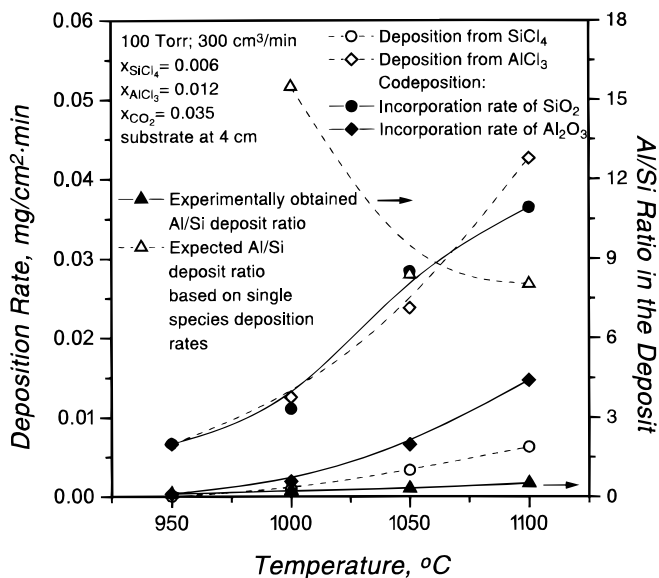


Figure 10. Effect of temperature on the rates of incorporation of Al₂O₃ and SiO₂ in the deposit and the Al/Si ratio at 100 Torr.

tions of Fig. 8. It is seen that the Al/Si deposit ratio increases with increasing distance from the entrance of the reactor, reaching a maximum close to the center of the hot zone. Since the maximum in the deposition rate and the maximum in the Al/Si ratio in the deposit occur at the about same position in the reactor (compare Fig. 8 and 11), one is led to conclude that high deposition rates promote the incorporation of Al in the deposit. The results of Fig. 11 suggest that it may be possible to circumvent the effects of the enhancement of the deposition rate of SiO₂ in the presence of AlCl₃ in the feed and obtain deposits with significant alumina and aluminosilicate (*e.g.*, mullite) content by manipulating the residence time of the reactive mixture in the reactor.

Silicon tetrachloride vs. MTS as silicon source gas.—It was mentioned in the introduction that in a past study²² we carried out a com-

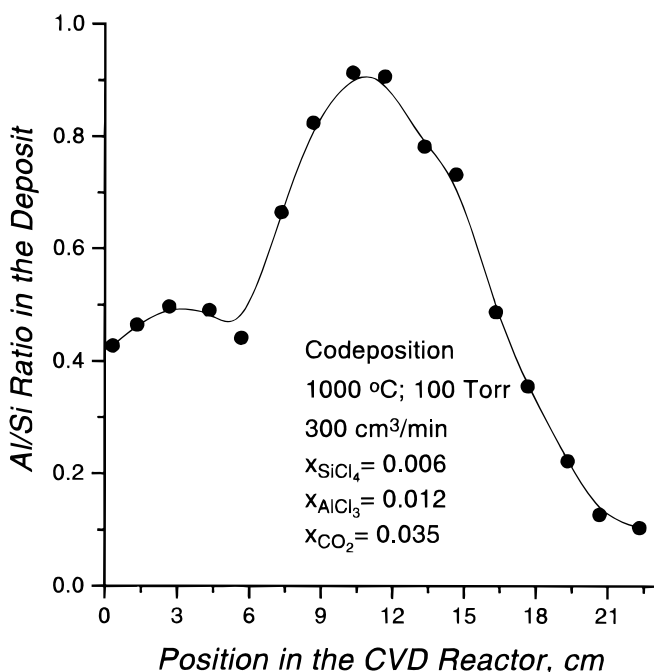


Figure 11. Al/Si deposit ratio vs. position in the reactor at the conditions of Fig. 8.

prehensive study of the deposition of silica, alumina, and aluminosilicates from mixtures of CH₃SiCl₃ (MTS), AlCl₃, CO₂, and H₂. Results from that study on the variation with the temperature of the codeposition rate and the deposition rates of silica and alumina in independent experiments are compared in Fig. 12 with deposition rate results measured when SiCl₄ is used as silicon source (Fig. 1). The comparison of the two sets of data reveals that when MTS is used as silicon source, both the deposition rate of silica and the deposition rate in the codeposition process are much higher (by almost an order of magnitude) than the corresponding values for SiCl₄ at all temperatures. It should be noted that with the exception of the mole fraction of CO₂ and the total pressure, the other operating parameters (chloride mole fractions, flow rate, and measurement location) do not have the same values in the two sets of data. However, as the results of Fig. 3-8 on the effects of these parameters on the codeposition rate and the deposition of silica show, the differences in Fig. 12 are much larger (by more than an order of magnitude in some cases) than the differences that would be expected from the different operating conditions and, in several cases, of the opposite sign. For example, as the results of Fig. 3 and 5 show, changing the SiCl₄ mole fraction from 0.006 to 0.011 (the MTS mole fraction in Fig. 12) would decrease both the codeposition rate and the deposition rate of silica at 1000°C and thus lead to larger differences between SiCl₄ and MTS as silicon source.

The apparent activation energies that are extracted for deposition of silica and aluminosilicate deposition (codeposition) from the results of Fig. 12 with MTS as silicon source (25.9 and 22.9 kcal/mol, respectively) are very close to the values found in this study for deposition from mixtures containing SiCl₄ [26.5 (excluding data below 925°C) and 22.1 kcal/mol, respectively (see Fig. 1)]. Even though apparent activation energies are influenced by several other factors in addition to the intrinsic kinetics of processes, the small differences in the activation energies for the two silicon sources offer a strong indication that the same controlling steps are probably involved in the deposition mechanisms of aluminosilicates and silica in the two cases.

It is possible to explain some of the differences that are observed in Fig. 12 between MTS and SiCl₄ using thermochemical equilibri-

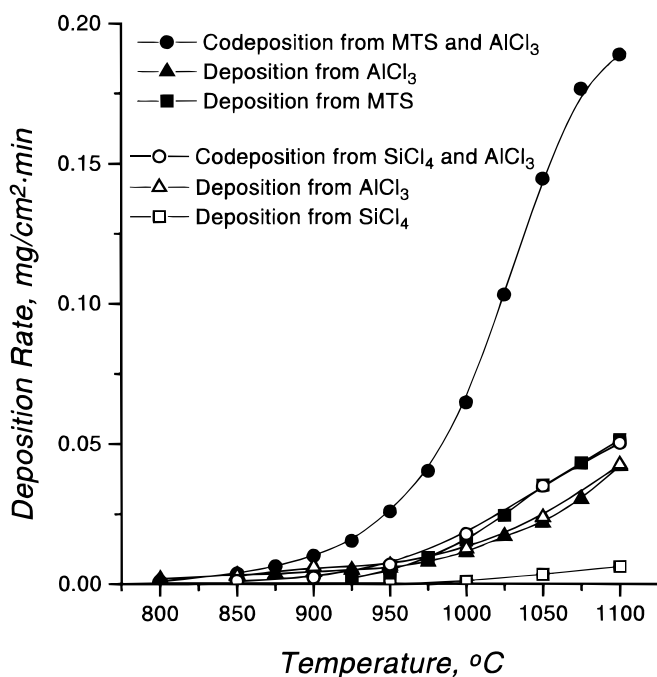


Figure 12. Comparison of deposition rates using MTS (●, ▲, ■) and (○, △, □) SiCl₄ as silicon source at 100 Torr and 3.5% CO₂. Other reaction conditions: (●, ▲, ■) 1.1% MTS, 0.9% AlCl₃, 250 cm³/min total flow rate, and substrate at 7 cm. (○, △, □) 0.6% SiCl₄, 1.2% AlCl₃, 300 cm³/min total flow rate, and substrate at 4 cm.

um analysis. Figure 13 presents results on thermochemical equilibrium in the Si/C/Cl/H/O system for elemental loadings corresponding to MTS-CO₂-H₂ (Fig. 13a) and SiCl₄-CO₂-H₂ (Fig. 13b) mixtures having the compositions used for deposition of silica in Fig. 12. Figure 14, on the other hand, presents results for thermochemical equilibrium in the Al/Si/C/Cl/H/O system for elemental loadings corresponding to the AlCl₃-MTS-CO₂-H₂ and AlCl₃-SiCl₄-CO₂-H₂ mixtures used for codeposition in Fig. 12 (Fig. 14a and b, respectively). More results on thermochemical equilibrium in silica, alumina, and aluminosilicate deposition with MTS as silicon source have been presented in Ref. 22. Only species having mole fractions larger than 10⁻⁶ are shown in Fig. 13 and 14, and the presented results refer to thermodynamic equilibrium with only gas-phase species allowed to

form. This was done because the quantities of material that must be transferred from the gas phase to the solid phase (*i.e.*, to the walls of the reactor) in order to establish complete gas-solid equilibrium are very large, requiring residence times that are several orders of magnitude larger than those prevailing in the experiments or in typical CVD reactors. A large database of gas-phase species with thermodynamic data compiled from various sources (see Ref. 22 and references therein) was used for the thermodynamic computations, which were carried out using a free energy minimization method.

The comparison of Fig. 13a and 14a with Fig. 13b and 14b, respectively, shows that even though the MTS mole fraction in the feed is by about a factor of 2 larger than the mole fraction of SiCl₄, the

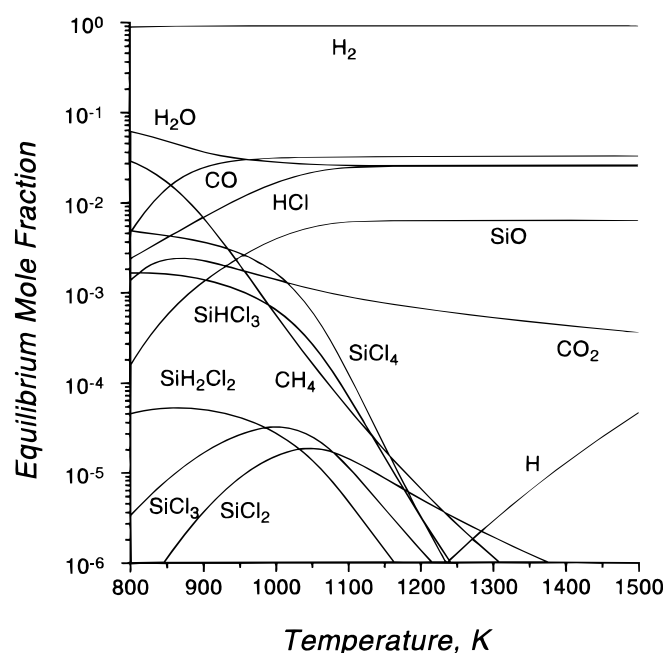
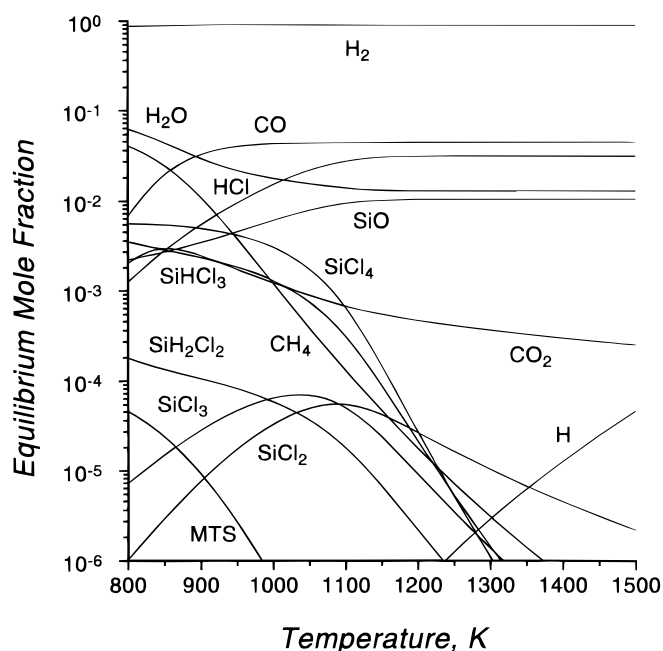


Figure 13. Equilibrium mole fraction vs. temperature for SiO₂ deposition at 100 Torr. Solid phases are not allowed to form. (a, top) CO₂/MTS = 3.3, $x_{\text{MTS}} = 0.011$; (b, bottom) CO₂/SiCl₄ = 5.8, $x_{\text{SiCl}_4} = 0.006$.

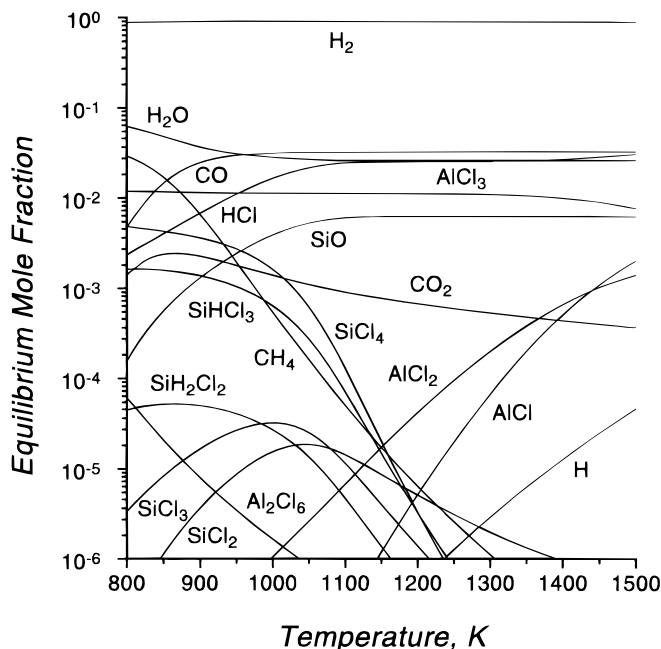
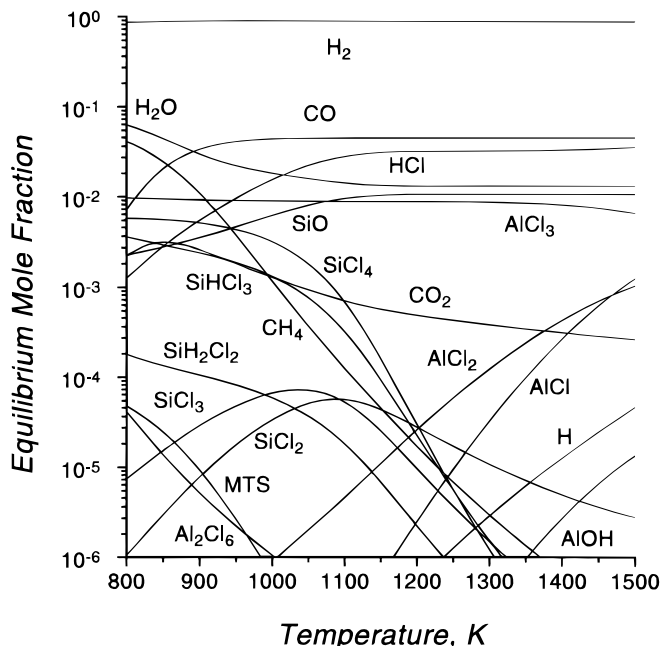


Figure 14. Equilibrium mole fraction vs. temperature for codeposition at 100 Torr. Solid phases are not allowed to form. (a, top) CO₂/AlCl₃/MTS = 3.3/0.8/1, $x_{\text{MTS}} = 0.011$; (b, bottom) CO₂/AlCl₃/SiCl₄ = 5.8/2/1, $x_{\text{SiCl}_4} = 0.006$.

mole fractions of SiCl_2 and SiCl_3 are almost an order of magnitude larger in Fig. 13a and 14a. These two radicals are the main products of silicon tetrachloride and MTS pyrolysis,^{25,26} and their high surface reactivity renders them the principal precursors for silica incorporation in the deposit. The thermodynamic equilibrium results of Fig. 13 and 14 are therefore consistent with the much higher deposition rates of silica and aluminosilicates when MTS is used as silicon source.

The introduction of AlCl_3 in the reactive mixture appears to affect insignificantly the fraction of HCl both for MTS and for SiCl_4 in the feed. The computation of thermodynamic equilibrium in the Al/C/Cl/H/O system (see results reported in Ref. 22) gave much lower mole fractions of hydrogen chloride at the conditions of Fig. 13 and 14. Since HCl is the main by-product of reactions forming alumina from AlCl_x and H_2O_2 species, this result can explain the suppression of the deposition of alumina when silicon chloride (MTS or SiCl_4) is added to the $\text{AlCl}_3\text{-CO}_2\text{-H}_2$ mixture. Figures 13 and 14 show that the introduction of AlCl_3 in the reactive mixture also has rather insignificant effects on the concentration of the various Si-containing species, such as SiCl_x . Therefore, the dramatic enhancement of the deposition of silica with the addition of AlCl_3 in the feed cannot be justified on the basis of thermochemical equilibrium analysis alone. It is believed that the increased rate of silica deposition is due to surface reaction steps involving aluminum and silicon species, adsorbed on the surface, whose main reaction product is silicon oxide. It is interesting to point out that studies on the codeposition of C and SiC from MTS and ethylene mixtures³¹ indicated that a similar interaction of silicon-containing species and carbon-containing species adsorbed on the deposition surfaces might be responsible for a dramatic enhancement of the deposition rate of carbon.

Conclusions

The chemical vapor codeposition of silica, alumina, and aluminosilicates from $\text{SiCl}_4\text{-AlCl}_3\text{-CO}_2\text{-H}_2$ mixtures was investigated in a subambient pressure hot-wall reactor by monitoring gravimetrically the deposition rate on small substrates. To determine the variation of the deposition rate and deposit composition with the location in the CVD reactor, deposition experiments were carried out on refractory wires placed along the center line of the reactor.

The results showed that both the codeposition rate and the single-oxide deposition rates were positively influenced by temperature. Similar values of apparent activation energy (around 20 kcal/mol) were determined for the three deposition processes for temperatures above 1000°C. The deposition rate of alumina and silica in independent experiments increased with increasing pressure for pressures between 75 and 300 Torr, but the codeposition rate exhibited local minima and maxima in the intermediate pressure range. The aluminum trichloride mole fraction had a positive effect on the rate of codeposition and the rate of alumina deposition. The effect of carbon dioxide mole fraction on the deposition rate was also investigated. The deposition rate vs. CO_2 mole fraction curves exhibited a maximum for all three deposition processes. The flow rate had a strong influence on the codeposition rate and the deposition rates of silica and alumina. The codeposition rate and the SiO_2 deposition rate were negatively affected by an increase in the flow rate, whereas the deposition rate of Al_2O_3 exhibited a maximum in its variation, the location of which was shifted to higher flow rates with increasing temperature. A maximum in the codeposition rate was also present at about the middle of the isothermal region of the CVD reactor.

The deposition of Al_2O_3 from mixtures containing AlCl_3 proceeded much faster than the deposition of SiO_2 from $\text{SiCl}_4\text{-CO}_2\text{-H}_2$ mixtures of comparable chloride concentration. When both chlorides were fed into the chemical reactor, the overall deposition rate (*i.e.*, the codeposition rate) was higher than the sum of the deposition rates of the simple oxides in the single-species deposition experiments at the same conditions for temperature above 950°C. The difference between the codeposition rate and the alumina deposition rate increased with increasing temperature and aluminum trichloride concentration. The elemental analysis of the codeposited films re-

vealed that in comparison to the rates seen in single-species deposition experiments, the codeposition process was characterized by a dramatic enhancement of the deposition of SiO_2 and a reduction in the deposition of Al_2O_3 . This result was in agreement with what was seen in a past study where methyltrichlorosilane was used as silicon source. However, in that case, the rate of silica deposition in single-species deposition experiments was much larger (by more than an order of magnitude), and the codeposition rate was by more than a factor of three higher than the sum of the deposition rates of the two oxides in independent experiments.

The morphology and the composition of the films were determined using SEM, XRD, and EDXA. The silica films were amorphous, and the alumina films consisted of $\kappa\text{-Al}_2\text{O}_3$ and $\theta\text{-Al}_2\text{O}_3$. These two alumina forms were also found to exist in codeposited films along with amorphous components. The analysis of the composition of composite films deposited on wires showed that the Al/Si ratio increased with increasing distance from the entrance of the reactor, reaching a maximum in the middle of the hot zone. The aluminum content of the codeposition product also increased with increasing temperature. These results indicate that it may be possible to obtain Al/Si deposit ratios that are close to that of stoichiometric mullite and alumina-rich mullite by manipulating the temperature of the reaction and the residence time of the mixture in the reactor.

Acknowledgment

This research was supported by a grant from the Department of Energy. The authors also acknowledge the help of Brian McIntyre of the Institute of Optics of the University of Rochester with the characterization of the films.

The University of Rochester assisted in meeting the publication costs of this article.

References

- J. E. Shelby, in *Treatise on Materials Science and Technology*, M. Tomozawa and R. H. Doremus, Editors, Vol. 17, pp.1-35, Academic Press, New York (1979).
- B. C. Gates, J. R. Katzer, and G. C. A. Schuit, *Chemistry of Catalytic Processes*, McGraw-Hill, New York (1979).
- I. Birkby and R. Stevens, *Key Eng. Mater.*, **122**, 527 (1996).
- E. Fredriksson and J.-O. Carlsson, *J. Chem. Vap. Dep.*, **1**, 333 (1993).
- R. Funk, H. Schachner, C. Triquet, M. Kornmann, and B. Lux, *J. Electrochem. Soc.*, **123**, 285 (1976).
- R. Colmet and R. Naslain, *Wear*, **80**, 221 (1982).
- K. N. Lee and R. A. Miller, *J. Am. Ceram. Soc.*, **79**, 620 (1996).
- D. R. Messier, and P. Wong, *J. Electrochem. Soc.*, **118**, 772 (1971).
- H. Altena, C. Colombier, and B. Lux, in *Proceeding of the 4th European Conference on Chemical Vapor Deposition*, J. Bloem., G. Verspui, and L. R. Wolf, Editors, Eindhoven, The Netherlands (1983).
- C. Taschner, B. Ljungberg, V. Alfredsson, I. Enderl, and A. Leonhardt, *Surf. Coat. Technol.*, **109**, 257 (1998).
- C. S. Park, J. G. Kim, and J. S. Chun, *J. Vac. Sci. Technol. A*, **1**, 1820 (1983).
- Y. W. Bae, W. Y. Lee, T. M. Besmann, O. B. Cavin, and T. R. Watkins, *J. Am. Ceram. Soc.*, **81**, 1945 (1998).
- S. W. Choi, C. Kim, J. G. Kim, and J. S. Chun, *J. Mater. Sci.*, **22**, 1051 (1987).
- R. Colmet, R. Naslain, P. Hagenmuller, and C. Bernard, *J. Electrochem. Soc.*, **129**, 1367 (1982).
- M. Ritala and M. Leskela, *Appl. Surf. Sci.*, **75**, 333 (1994).
- E. Sipp, F. Langlais, and R. Naslain, *J. Alloy Compd.*, **186**, 65 (1992).
- S. Kim and G. R. Gavalas, *Ind. Eng. Chem. Res.*, **34**, 168 (1995).
- S. M. George, O. Sneh, A. C. Dillon, M. L. Wise, A. W. Ott, L. A. Okada, and J. D. Way, *Appl. Surf. Sci.*, **82/83**, 460 (1994).
- R. Mulpuri, Ph.D. Dissertation, Boston University, Boston, MA (1996).
- M. Auger and V. K. Sarin, *Surf. Coat. Technol.*, **94-95**, 46 (1997).
- K. Itatani, T. Kubozono, F. S. Howell, A. Kishioka, and M. Kinoshita, *J. Mater. Sci.*, **30**, 1158 (1995).
- S. F. Nitodas and S. V. Sotirchos, in *Chem. Vapor Dep.*, **5**, 219 (1999).
- G. D. Pappasoulis and S. V. Sotirchos, *J. Electrochem. Soc.*, **142**, 3834 (1995).
- J. G. Kim, C. S. Park, and J. S. Chun, *Thin Solid Films*, **97**, 97 (1982).
- P. Gupta, P. Coon, B. G. Koehler, and S. M. George, *Surf. Sci.*, **249**, 92 (1991).
- D. Woiki, L. Catoire, and P. Roth, *AIChE J.*, **43**, 2670 (1997).
- K. S. Kim, *AIChE J.*, **43**, 2679 (1997).
- J. W. Klaus, A. W. Ott, J. M. Johnson, and S. M. George, *Appl. Phys. Lett.*, **70**, 1092 (1997).
- M. L. Wise, O. Sneh, L. A. Okada, and S. M. George, *Surf. Sci.*, **364**, 367 (1996).
- V. J. Silvestri, C. M. Osburn, and D. W. Ormond, *J. Electrochem. Soc.*, **125**, 902 (1978).
- S. V. Sotirchos and I. Kostjulin, *Ceram. Trans.*, **79**, 27 (1996).